WPMST1-PR(18) 21223

P.T. Lang et al.

Plasma composition control by mixture pellets at ASDEX Upgrade

Preprint of Paper to be submitted for publication in
Nuclear Fusion

This work has been carried out within the framework of the EUROfusion Consortium and has received funding from the Euratom research and training programme 2014-2018 under grant agreement No 633053. The views and opinions expressed herein do not necessarily reflect those of the European Commission.

Plasma composition control by mixture pellets at ASDEX Upgrade

P.T. Lang[1], A. Drenik[1], R. Dux[1], T. Jackson[2], O.J.W.F. Kardaun[1], R.M. McDermott[1], B. Ploeckl[1], M. Prechtl[3], V. Rohde[1], R.R. Ruess[3], P.A. Schneider[1], M. Schubert[1], G. Tardini[1], ASDEX Upgrade Team

1) MPI für Plasmaphysik, Boltzmannstr. 2, 85748 Garching, Germany
2) CCFE, Culham Science Centre, Abingdon, Oxon, OX14 3DB, UK
3) Hochschule für angewandte Wissenschaften Coburg, Friedrich-Streib-Str. 2, 96450 Coburg

Abstract
Experiments were performed that aimed to control the plasma isotopic mixture by delivering supplemental components into the plasma via pellet injection. Pellets, mm sized solid bodies of frozen fuel, are either formed from a mixture of different hydrogen isotopes or from deuterium (D) with added elements. Mixed HD pellets were produced reliably and reproducibly providing the required 1:1 ratio of the protium (H) and D, mimicking the situation in a future fusion reactor with D and tritium (T). By applying pellet fuelling, control of the plasma isotope composition was established while gaining access to the reactor-relevant high-density regime and though to demonstrate mainly the controlling capability. Experiments provided information on the impact of the isotopic composition on the plasma performance. There is a strong indication that adding H to a D reference plasma causes a reduction of both the particle and energy confinement. The deleterious impact of H on the particle confinement is, apparently, even stronger than on the energy confinement. Furthermore, small amounts of H can cause a loss of energy confinement that is stronger than anticipated by the H98(y,2) scaling which is usually employed in reactor design studies. In the course of this experiment, pellets were demonstrated to be an effective and powerful tool for detailed investigations of the isotope effect. A first test demonstrated that producing and launching pellets that contain a mixture of different elements is a feasible technique. The latter was achieved by doping a D host pellet despite technical reasons limiting the permissible amount of processed N.

1. Introduction

The function of core particle fuelling in the next-step experimental reactor-scale tokamak device ITER and in the planned demonstration fusion power plant EU-DEMO [A] is by no means a trivial one. Injection of pellets, cryogenic mm size bodies of solid fuel, taking place at high speed from the magnetic high-field side into the plasma column is expected the most suitable approach for this task. Currently, this technique is regarded as the sole option to meet the multiple requirements for fuel delivery (at the needed quantity and quality) sufficiently deep inside the core plasma [B]. Applying the pellet tool it is aimed to achieve a central density close to or even beyond the Greenwald density n_{Gw} [C] while keeping the edge density sufficiently low. When simple gas-puff fuelling is applied, in tokamaks the Greenwald density, originally derived for L-mode and Ohmic discharges [C], is commonly recognized as a rather general empirical density limit. When operating in the high confinement regime (H-mode) even more severe limitations are faced [D]. Occasionally spontaneous density profile peaking was observed, under specific conditions, at DIII-D which resulted in operation above the Greenwald density while maintaining good energy confinement [E]. The deadlock mostly faced with gas fuelling was found to be released by pellet fuelling. This was attributed to different behaviour with respect to conditions in the plasma edge. Recent experiments demonstrated core density control at a reactor grade level of about 1.25 n_{Gw}, while keeping the H-mode [F]. Hence, pellet core particle fuelling can be considered as an essential technique of nuclear fusion; however, a couple of physics and technology issues still need further consideration. Contrary to present-day research devices, regulatory safety restrictions and economical aspects will become major factors restraining the design of commercial fusion power plants. As a consequence, the total inventory of tritium (T) must be as low as reasonably possible, while the effort for processing the exhaust gas has to be kept at a bearable level [G]. This exhaust gas will be composed of unburned fuel, T and deuterium (D), as well as the fusion “ash” helium (He). For operational reasons it is also likely that additional gases have to be inserted into the reactor vessel in order to dissipate radiative power and enhance plasma performance. Finally, e.g. to maintain an economically reasonable design of the protium (H) removal system in the EU-DEMO fuel cycle, a low fraction of H to the total number of plasma particles has been mooted as acceptable [G]. As a consequence, the pumped exhaust gas will be a multi-species composite, subject to handling within the fuel cycle. Ultimately, also the fuel delivered as input for the pellet launching system (PLS) will likely consist of several components, rather than of pure D and/or T. It is understood that the processing of the gas mixture provided to the PLS has to guarantee that all key task requirements can still be fulfilled. However, it is worthwhile to consider whether injection of composite pellets formed from a gas mixture (e.g. D, T, Ne, Ar), exhibit specific advantages, both for the pellet injection performance and the efficiency of the fuel cycle.

In this paper, we pursue two different ideas. The first one, representing the major part of this investigation, refers to the approach to control isotope mixture in the plasma centre directly via the pellet isotope mixture. Evidently, our experiments performed at the tokamak ASDEX Upgrade (AUG) employed a mixture of H and D, which mimics the fuel composed of D and T in a reactor. Data from these experiments were employed to study the isotope effect. The second idea, which is discussed only briefly in this paper, considers the production and application of pellets doped with additional elements. In the example shown, we added a small amount of nitrogen (N). N is widely-used in AUG anyway, as it was found to be an efficacious plasma enhancement gas (PEG) improving the plasma energy confinement [H].

2. Set-up

The set-up employed in the present investigation is very similar to that employed in a recent study where more details can be found, see [F]. Here, some basic elements are briefly repeated and supplementary information on issues specific for this investigation is provided.

AUG is a mid-size divertor tokamak (major radius $R_{maj.}$ = 1.65 m, minor radius a_{min} = 0.5 m) with a reactor-relevant all-metal-wall configuration. It is equipped with a versatile auxiliary heating system, a broad set of diagnostics that enable sophisticated investigations as well as an elaborated discharge control system (DCS); however the device is not designed for T handling. The pellet launching system allows for reactor relevant and efficient pellet injection from the torus inboard side at repetition rates up to 83 Hz providing pellets of variable particle contents m_P and speeds v_P. Applied pellet parameters m_P and v_P are pre-selected and fixed for every discharge; the pellet frequency f_P is employed to control the pellet particle fluxes $\Gamma_P = m_P \cdot f_P$, because pellet acceleration takes place in a stop-cylinder type centrifuge [I] that rotates at a preselected revolution rate f_C, $f_P = f_C/n$ with n integer. Thus, only a discrete spectrum of f_P and Γ_P values is available. Pellet production takes place in a batch process. Ice rods with a preselected cross section are extruded from a reservoir into a storage cryostat where they are kept until pellets are cut on request, accelerated and guided into the torus. Due to the finite length of the stored ice rod, the amount of available pellets per discharge is limited (in the case of large size fuelling pellets) to 96. Initially, the system was designed to handle either high purity H_2 or D_2 for the ice formation. Recently, gas handling and extrusion control capabilities have been improved in order to create and handle gas mixtures [J]. In this study, we made use of this facility to produce ice from a mixture of H_2 and D_2 gas, which was taken from a high pressure bottle initially filled with H_2 and D_2 gas at ratio 1:1. Since the bottle was stored afterwards for several months allowing for HD formation by isotope exchange reactions, samples of the actual gas composition were taken and analysed in a stationary high-resolution mass spectrometer. Absolutely calibrated residual gas analysers (RGAs) survey the residual gas pumped from the vacuum vessel at different toroidal locations at the inner and outer divertor and the outer mid plane. For the analysis of the isotope ratio, a fitting routine was used [K,L] on the RGA data. The routine is based on a model [M] defining a probability distribution for all of the possible hydrogen isotopologues of a molecule, based on its average hydrogen isotope ratio. A common signal of the hydrogen isotope ratio is created by averaging over the isotope ratios reported by the RGAs at different locations.
The H:D ratio in the edge and divertor region was determined from Balmer spectra that were measured on 5 lines-of-sight which cross the inner and outer divertor leg. The spectra of the Balmer-δ lines (transition n = 6 → n=2) of H (at 410.174 nm) and D (at 410.063 nm) and of the Balmer-ε lines (transition n=7 → n=2) of H (at 397.008 nm) and D (at 396.904 nm) were recorded with 4 ms temporal resolution. The spectra were fitted taking the Stark broadening of the corresponding lines into account [N]. The ratios of the line radiances L were used to calculate the H-fraction H/(H+D), i.e. $\frac{L_{H\delta}}{L_{H\delta}+L_{D\delta}}$ and $\frac{L_{H\varepsilon}}{L_{H\varepsilon}+L_{D\varepsilon}}$. The H-fractions obtained from the two lines agreed within statistical uncertainty, the estimated standard deviation of H/(H+D) varying between 0.02 and 0.04.
To obtain information on the H:D ratio for the core plasma, the thermal neutral fluxes are measured with an E-M mass spectrometer type neutral-particle analyser (NPA), see [O]. The neutrals that leave the plasma and are measured by the NPA originates from plasma ions and from background neutrals. Therefore, they contain information about the plasma composition.
The neutron yield turned out to be a useful indicator of the H:D ratio in our investigations, it is measured with an absolutely calibrated array of five detectors which cover a wide range of count rates, see [R].

3. Qualifying the HD pellet actuator

In a first step, the pellet actuator was commissioned to control the H:D isotope mixture in the AUG plasma. Ultimately, the goal is to achieve and keep an equipartition of H and D in the plasma centre; however, yet a real-time measurement that enables feedback actuation is still lacking. Instead, a feed-forward hit-or-miss test was envisaged by choosing a 1:1 ratio for the

pellet HD fuel, in spite of the fact that this is not expected to be precisely the required composition in the plasma, due to different particle sustainment times of both species.
A bottled gas mixture was procured, formed by high-purity H_2 and D_2 molecules in a ratio of 1:1. In such a gas mixture, due to isotope exchange reactions, HD molecules are gradually formed and finally a composite mixture of three isotopologues with a H_2:HD:D_2 ratio of 1:2:1 is approached, see [S]. For the predominant conditions in the bottle, reaction rates are rather low. Hence, the amount of HD molecules increases only slowly. Mass spectrometric analysis of the gas in advance of the investigations showed that, in our initial gas mixture, the fraction of HD molecules was only 1.2 %. Although the HD formation does not alter the H:D ratio, the handled gas mixture was composed of 3 hydrogen isotopologues. Correspondingly, the main process parameters (temperature and pressure) for the freezing, annealing and extrusion of the ice had to be adapted for this mixture. It turned out that their progression at about 15 K is closer to those elaborated for pure D_2 (at 17 K) rather than for pure H_2 (at 10 K). However, the acceptable temperature range turned out to be much narrower than for the mono isotopic cases; hence the HD handling required higher processing precision. Nevertheless, after some experimentation, reliable and reproducible formation of intact and stable HD ice could be achieved and the pellets launched were found to be suitable for our purposes.

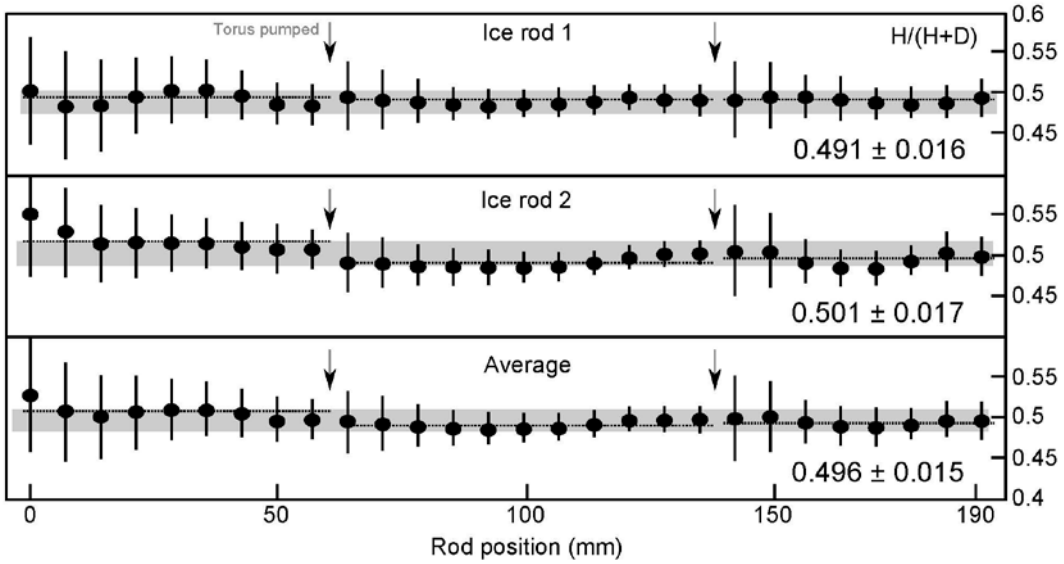

Figure 1: Analysis of the H/(H+D) composition of two ice rods produced from an initially 1:1 H_2/D_2 gas mixture. Consecutive sequences of 3 pellets were launched into the torus, after each sequence the residual gas was analysed. After several sequences, the torus had to be re-evacuated, thus 3 rod sections are analysed separately. Dashed lines represent the average isotope composition of the three sections.

The first topic of our investigation was the characterisation of the pellet actuator. This was done by injecting the HD pellets into the pre-evacuated torus, surveying the released gas with the RGA. Results achieved by injecting (fuelling sized) pellets which consumed two entire 192 mm long ice rods are shown in figure 1. Consecutive sequences of 3 pellets were launched into the torus; after each sequence the residual gas was analysed. After several sequences, the torus had to be re-evacuated, thus 3 rod sections are analysed separately. For both rods the results are shown in a separate box, a spatial average overlaying these data is displayed in the lower box. The dashed lines represent the average isotope composition of the three sections; values displayed an error-weighted average of all data displayed in the box. In fact arriving pellets show a H:D ratio very close to 1:1; obviously neither ice production nor pellet transfer did alter the initial ratio. However, compared to the initial gas analysis, a

significantly higher fraction of HD molecules was found by the RGA. This is attributed to reactions at the wall of the plasma vessel.

4. Actuation on the H/(H+D) ratio

The next step was to sound out the efficacy of the HD pellets for isotope mixture control. For this we selected a scenario used in a previous investigation on feedback-controlled high-density operation, see [F]. The scenario was chosen to robustly handle strong pellet-particle fluxes that result in a high core density. Hence, it is most suitable for the present investigations, although it did not yield a high performance in global plasma energy confinement. In addition, a few discharges performed using pure D for all relevant actuators could be utilised as valuable reference, in order to analyse the impact of adding H. These three discharges were all run with the same plasma current I_P = 0.8 MA, toroidal magnetic field B_t = 2.5 T, edge safety factor q_{95} = 5.3, plasma volume V_p = 12.7 m^3, elongation κ = 1.68 and upper and lower triangularities δ^u = 0.14 and δ^l = 0.43, respectively. H-Mode conditions were established and maintained by steady auxiliary heating, relying mainly on neutral beam injection (NBI) but employing as well wave heating of the core in order to prevent impurity accumulation. In the D references (D pellets into D plasma), 3 NBI sources (D^0 injection at 60 kV respectively 90 kV) with each source delivering about 2.5 MW were employed, supported by up to 4 MW ion cyclotron resonance heating (ICRH) at 36.5 MHz. In the HD discharges, 4 NBI sources (H^0 injection at 50 kV and 70 kV, respectively) with each source delivering up to about 1.8 MW were employed; however since ICRH was hampered here by the presence of H it had to be substituted by electron cyclotron resonance heating (ECRH) at 140 GHz. To cope with the resulting high densities, the polarisation of the ECRH was changed from X-2 mode into O-2 mode shortly before pellet injection in view of its higher cut-off density. In addition, to guarantee proper ECR absorption, the core temperature was intended to be kept above 3keV. (Occasionally, during high flux phases, core temperatures dropped to about 2keV.) At the time of these experiments the available ECRH power in O-2 mode was restricted to about 1 MW. Therefore, in order to avoid losing efficient core heating and/or suffering from impurity accumulation in the core, the pellet rates were increased carefully step by step. The maximum available pellet rate was only applied once, briefly at the very end of the pre-programmed sequence.

The basic aim of these experiments was to replace the initial gas puff gradually by the HD pellets and study the impact on the plasma isotope mixture. From the D reference discharges it became clear that during pellet actuation the edge density must be kept at a constant level, in order to avoid a loss of energy confinement. Evidently, this can best be achieved by feedback-control acting simultaneously on gas and pellets, which finally implies density profile control. However, here higher priority was put to study the actuator impact and hence gas and pellet fluxes were kept constant for fixed periods yielding a stable H:D ratio in the applied fuelling flux. Consequently, pre-programmed feed-forward requests were executed by the gas puffing system and the PLS. The stepwise increase of the pellet flux was anticipated by an approximately compensatory reduction of gas puff. Laid out for studying the actuation, these experiments were not optimised for physics investigations with respect e.g. to the isotope effect on the plasma performance.

As well as for D pellet fuelling, HD pellet actuation proved most suitable for operation at high density. Due to its higher fuelling efficiency with respect to gas puffing, replacing gas on par with pellet fuelling results in a significantly higher density. This can be seen from figure 2, showing a discharge of the series where HD pellets were employed. Displayed there are the applied auxiliary heating power and the radiation (box (a)), the plasma stored energy (b), the centre density from the Thomson scattering system (TS) (red diamonds) and the line averaged density derived in real time from a simple algorithm employing measurements from the laser interferometer and the Bremsstrahlung, see [T], (box (c)), the centre temperature from TS (d),

the gas and the pellet particle flux (e) and the ratio H/(H+D) from divertor spectroscopy as well as from NPA (f). It is obvious that both line-averaged and central densities increase with increasing pellet fuelling. During phases of almost constant particle flux, the energy confinement is also almost constant. The final part of the discharge with reduced fuelling showed higher confinement, but this situation is very prone to core impurity accumulation and hence not suitable for steady operation. Yet, despite the limited power, core ECRH turned out to be sufficient to avoid this. During the pellet phase a moderate gradual decrease of the impurity content (B, C, N and W monitored) is observed. This decrease, however, does not influence the radiative losses significantly and is mainly attributed to a reduced impurity influx after forming an X-point configuration. In a short concluding pellet sequence, while applying maximum flux, the density profile is somewhat peaked, while the central density reaches the Greenwald density. Next-step investigations should thus envisage applying feedback control of the core density.

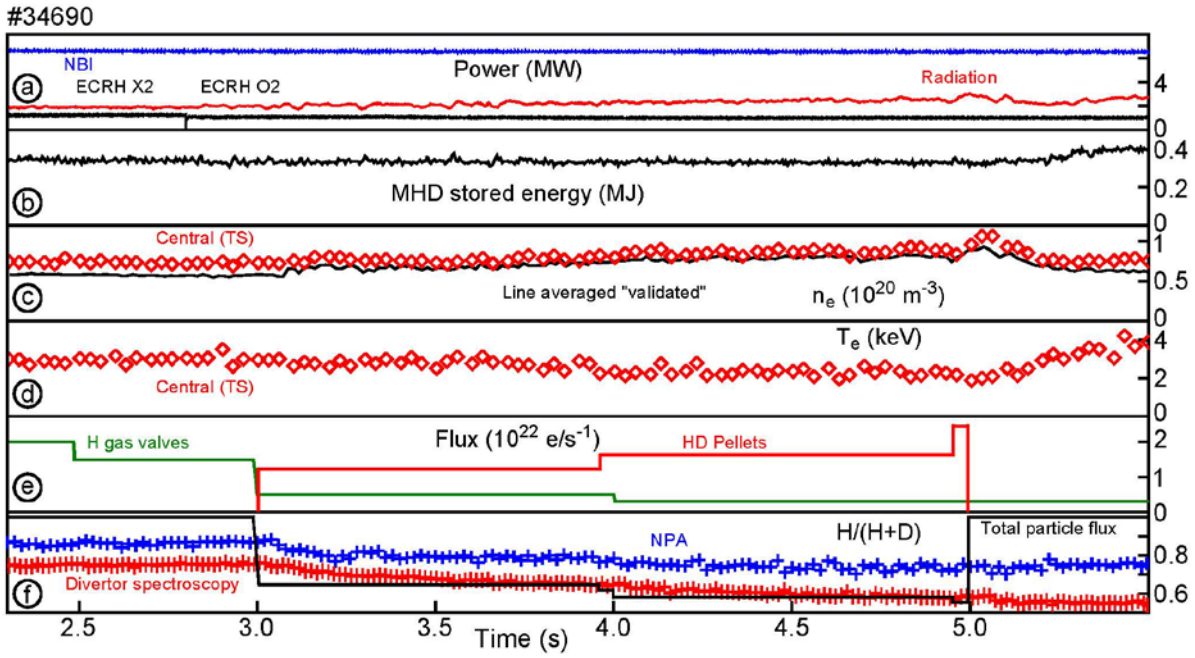

Figure 2: Overview of a typical plasma discharge testing the isotopic fraction control by H/D-pellet injection. In this case, a pure H gas puff is gradually replaced by HD-pellets. This results in a considerable decrease of the H fraction in the plasma. Due to the higher fuelling efficiency, both line-averaged and core density are increased by the pellets. The plasma stored energy remains unaffected while the temperature is decreased. The pellet sequence is concluded by a short phase with maximum pellet flux which generate a short high-density phase that reaches the Greenwald density in the plasma centre.

The discharge shown and discussed so far was only one of a series of three consecutive ones, applying the HD pellets in different combinations of the initial gas puff. The experiment was performed right after a phase of D plasma operation during the transition towards H plasma operation. To prepare for H operation, glow discharges in H were run in order to reduce the D content of the wall. Nevertheless, conditions with respect to the wall loading by H and D have still been transient and are not fully consistent with the aim of our approach. In every discharge, the strong initial gas puff was replaced in several steps by the HD pellets, keeping the total particle flux approximately the same. In the first discharge, the gas puff was purely D_2. Pure H_2 gas was puffed in the second shot. This is the discharge shown in figure 2, which contains a short final phase in the pellet sequence. Here, the maximum f_P was applied to gain access to very high densities. In the last shot, which aimed at establishing a plasma with the

desired isotope mixture, both H_2 and D_2 gas were puffed at a ratio of 1:1. Results are shown in figure 3, which displays the temporal evolution of the three cases. Upper boxes show the particle fluxes from the gas valves (blue D_2, green H_2) and from the pellet launcher (red, calculated from set parameter). In the lower boxes the H/(H+D) fraction as calculated from the total particle flux (consisting of both gas and pellets) is plotted as a solid grey line. This parameter is displayed as "measured by spectroscopy". The corresponding diagnostic observed the divertor region (indicated by red crosses). It is noted that the spectroscopy results are in very good agreement with the RGA data, the latter of which provides less temporal resolution.

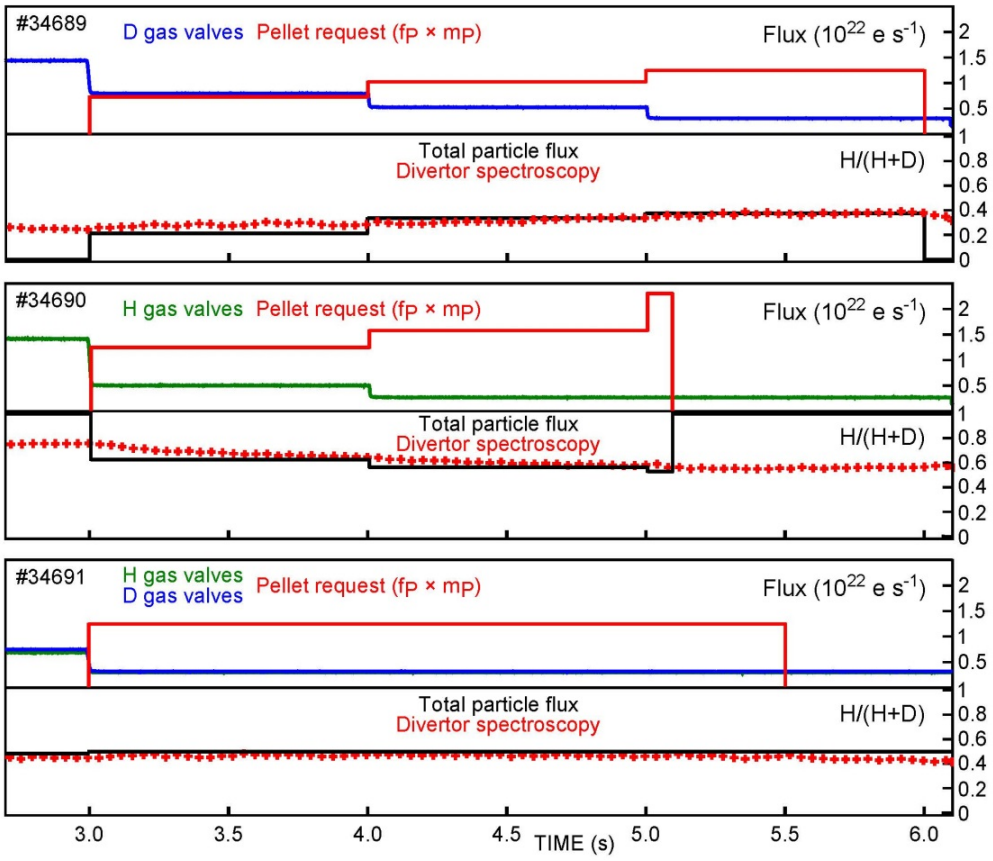

Figure 3: Adjusting the H/(H+D) isotope fraction by injection of H/D pellets replacing the initial strong gas puff. In case a pure D gas puff is replaced, the H content is increased; H gas puff replacement reduces the H content. For sufficiently strong particle fuelling, the isotopic fraction measured by divertor spectroscopy approaches quickly the total flux fraction.

During the first two shots the pellet actuator definitely provides its key feature by changing the isotopic ratio in the requested manner. In the third case, the isotopic ratio established during the initial gas phase is virtually unaffected by the switch to pellet fuelling. In the initial phases and also during phases with a low particle flux there are cases where the isotope mixture of plasma and applied flux deviate significantly. This is attributed to a wall reservoir not yet fully equilibrated. However, once a sufficiently high flux is applied – either by gas, pellets or a combination of both – the plasma H/(H+D) fraction approaches the target value within about 1 s. For the discharges performed here, even the 1:1 hit-or-miss choice made for the isotopic ratio in this first test turned out to be suitable for establishing the required plasma isotope composition.

5. Analysis of the H/(H+D) ratio

In order to achieve full control of the plasma isotope mixture, knowledge of the plasma composition is required in real time. Yet, such data are not routinely available. Corresponding efforts are now under way; during the present study various available diagnostic systems have been adapted to this task. Hence, cross checking of their results is part of this investigation, too. In the following, the isotope ratio is represented by the hydrogen fraction H/(H+D).

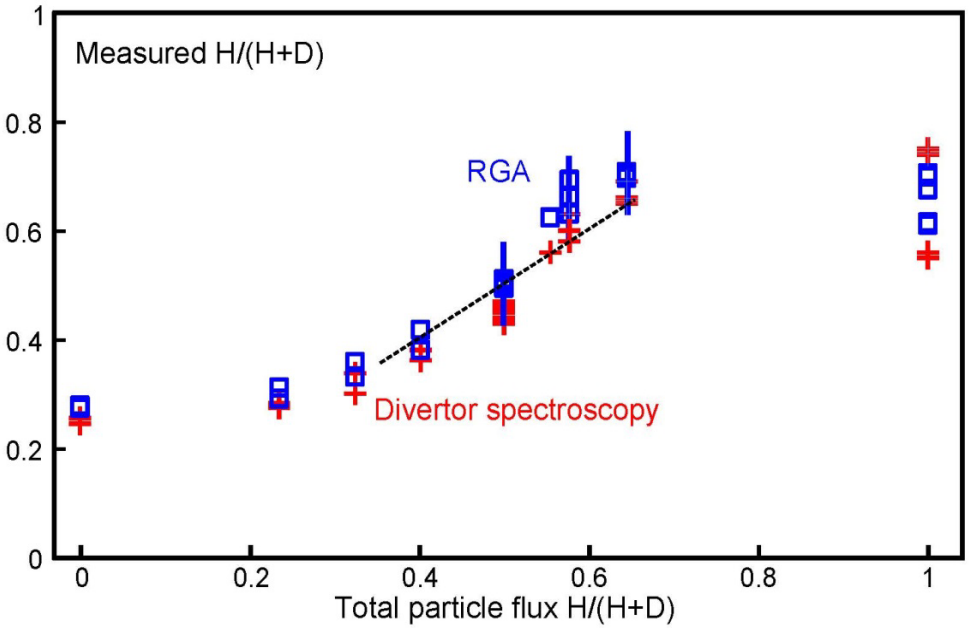

Figure 4: H/(H+D) ratio as measured by divertor spectroscopy and the RGA versus the applied one in the fuelling flux (gas & pellets). Both measurements agree quite well within the accuracy range (indicated by vertical bars for the RGA data). Within the region of almost balanced isotope distribution (dashed line), the requested plasma composition is matched fairly well.

5.1. Edge and divertor region

The data from spectroscopy and RGA were made available already shortly after a discharge. Therefore, the diagnosis of the plasma edge and divertor region turned out to be straightforward and reliable. In addition, within their specified range of reliability, both measurements agree very well, which can be seen from figure 4. This figure displays the H/(H+D) ratio (measured directly by divertor spectroscopy and RGA), plotted versus the estimated total particle flux. The latter was calculated by gas fluxes that were delivered via valves from different H and D reservoirs, and by estimating the applied pellet flux based on the requested rate and while assuming H/(H+D) = 0.5 for the pellets. As indicated by the dashed line, evidently in the region of interest, H/(H+D) about 0.35 to 0.65, the estimated applied total flux ratio very well matches the measured one. For this region (with an almost balanced isotope distribution) all the data shown in figure 4 refer to phases where a significant flux is applied. For cases with one of the two isotopes used solely or as dominating majority, significant deviation is found between particle flux and the isotope mixture of the edge plasma. Most of these data correlate to phases with low flux rates (as discussed before), and are thus attributed to the influx from a not yet fully equilibrated wall reservoir. Hence, with respect to the isotope composition of the target plasma in the edge and divertor region (where reliable data are available), this first control approach turned out to work fairly well when

sufficient flux was applied. Aiming at high density operation, the latter condition is to be fulfilled anyway.

5.2. Core plasma

The reactor relevant region of interest for isotope control is unquestionably the plasma centre. Due to differences in the transport properties of the different hydrogen isotopes, the ratio occurring at the plasma edge will not necessarily be the same as the ratio in the centre. The H/(H+D) core ratio however cannot be directly measured, but needs a sophisticated analysis of the data. Subsequent to the first isotope-control experiment, an analysis of NPA data and the neutron rate was performed to obtain information about the H/(H+D) ratio in the core region. In addition this investigation might foster the development of these diagnostics towards a serviceable control tool.

5.2.1 NPA

The fluxes of neutral H and D measured with the NPA carry information about the isotope composition of the core plasma. The reconstruction of birth profiles from the measured neutral fluxes needs to take the different mean-free paths of H and D into account. The mean-free path was determined by simulating the attenuation of neutral fluxes due to charge exchange and ionisation with the NPA model, see [P] of the 3D Monte Carlo code FIDASIM [Q]. To obtain information about the plasma core it is beneficial to analyse the high-energy tail of the velocity distribution of the thermal particles. Particles with higher energies originate from farther within the plasma. However, since the observed plasmas are heated by neutral beam injection, the velocity distribution at high energies is dominated by beam particles. In the presented case, the highest energy not significantly perturbed by beam particles is 2 keV. The simulated radial birth profile for this energy is shown in figure 5 for a pure H and a pure D case.

By taking the birth profiles for different isotopes into account, one can reconstruct the expected isotope composition of the plasma. This is shown in figure 6 by black circles. The ratio of measured neutral fluxes (grey circles) would suggest an isotope composition which is between 1.1 and 1.3 above the just described model, which is considered to be more realistic. This deviation, determined for the plasma parameters in this particular experiment, is expected to change with collisionality. The (weighted) average birth position of the neutrals is near a normalised poloidal radius $\rho_{pol.} \sim 0.9$, and therefore, well within the pedestal top. This observation suggests a higher fraction of H in the confined plasma than observed in the SOL. The reason for this difference is still under investigation.

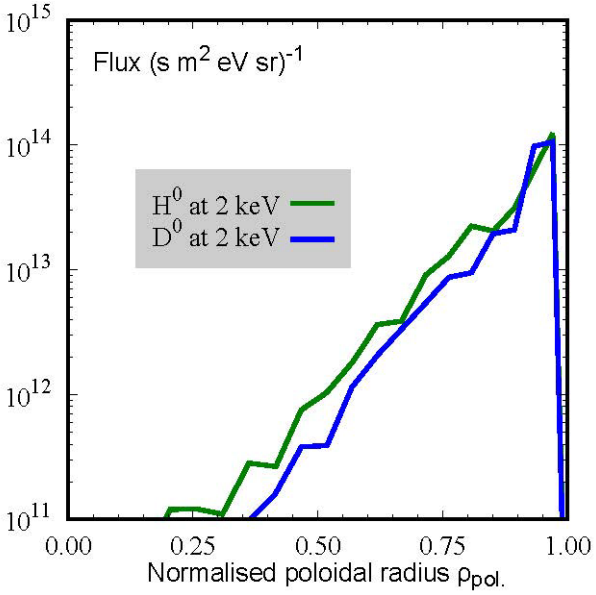

Figure 5: Birth profiles of neutral particles for a pure H and a pure D plasma simulated with FIDASIM using the plasma parameters of discharge #34689.

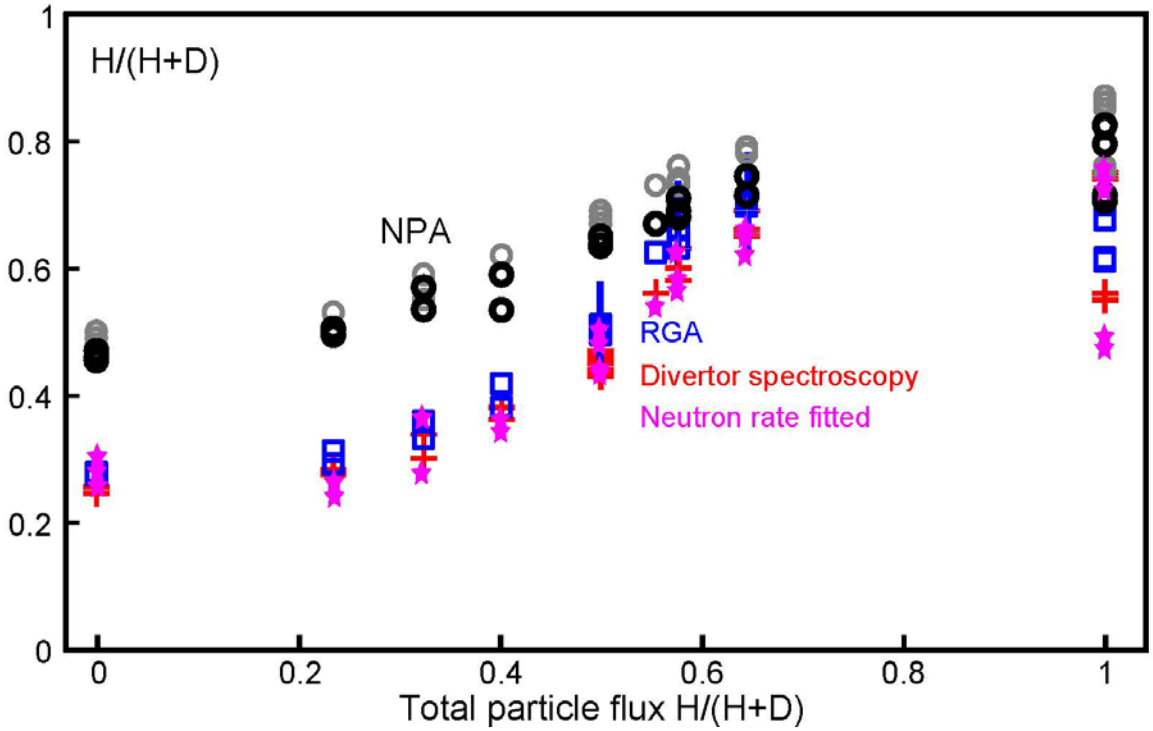

Figure 6: Directly measured H/(H+D) by the NPA (grey circles) and values calculated taking into account CX probabilities and attenuation (black circles) in comparison to edge diagnostics data. Added as well are data estimated from the neutron rate calibrated to fitted relation (*).

5.2.2 Neutron rate

Since only H^0 beams have been injected in the HD control approach discharges, no beam-target reactions usually providing the major component of neutron production in AUG took place. Therefore, and because of the high H fraction, the only essential contribution in these discharges is from thermal particles producing neutron rates that are about 1000 times lower than in the reference discharges heated by D^0 NBI (several 10^{11}/s instead of several 10^{14}/s).

Despite the rather low intensity, the neutron rate was found to be utilisable for checking the H/(H+D) ratio determined from the other methods as discussed previously in this chapter. According to [U, R], the thermal neutron rate S_{th} is (approximately) proportional to

$$S_{th} \sim {T_i}^2 \, {n_D}^2$$

with T_i the ion temperature and n_D the D density. Assuming equal ion and electron temperature, $T_e = T_i$, which is usually well justified for high densities and disregarding profile changing effects, we used the quantity

$$\hat{S}\,(J^2) = \left[W_{MHD}\,\left(1 - \frac{H}{H+D}\right)\right]^2 \quad (*)$$

as a measure for the predicted neutron rate in order to compare it with the measured neutron rate. This is done with respect to a fixed data set where the ratio H/(H+D) has been estimated in several ways. Specifically, the ratio has been calculated from:

(I) Total applied particle flux (gas & pellets)
(II) Total applied particle flux (gas & pellets) restricted to H/(H+D) values within the range 0.35 – 0.65
(III) Divertor spectroscopy measurements
(IV) RGA measurements
(V) Divertor spectroscopy & RGA measurements
(VI) NPA flux ratio measurements
(VII) NPA (modelled)
(VIII) Divertor spectroscopy measurements & NPA (modelled)

For each of these 8 replication sets the analysis was performed assuming a linear regression model on normal scale without intercept.
Result are shown in table 1, displaying the product-moment correlation coefficient R with respect to the fitted regression function and corresponding 95% confidence interval estimates based on Fisher's Z-transformation, see e.g. [V], as well as the regression coefficient c for every replication set. Each replication set contains 31 data points, except for the restricted total flux set which contains only 19 observations.

Replication data set	R	95% confidence interval	$c\left(\frac{1}{J^2 s}\right)$
Total flux	0.26	0.20-0.73	10.5
Total flux – restricted range	0.922	0.90-0.984	17.0
Spectroscopy	**0.953**	**0.95-0.988**	**15.0**
RGA	0.930	0.93-0.982	16.1
Spectroscopy & RGA	0.946	0.94-0.987	15.5
NPA measurements	0.853	0.85-0.962	36.2
NPA modelled	0.907	0.90-0.976	31.2
Spectroscopy & NPA modelled	0.943	0.94-0.986	21.0

Table 1: Empirical correlation coefficients R, with respect to the fitted regression line, 95% confidence interval estimates and regression coefficients c estimated from 8 different replication data sets that are based on varying methods to obtain the H/(H+D) ratio.

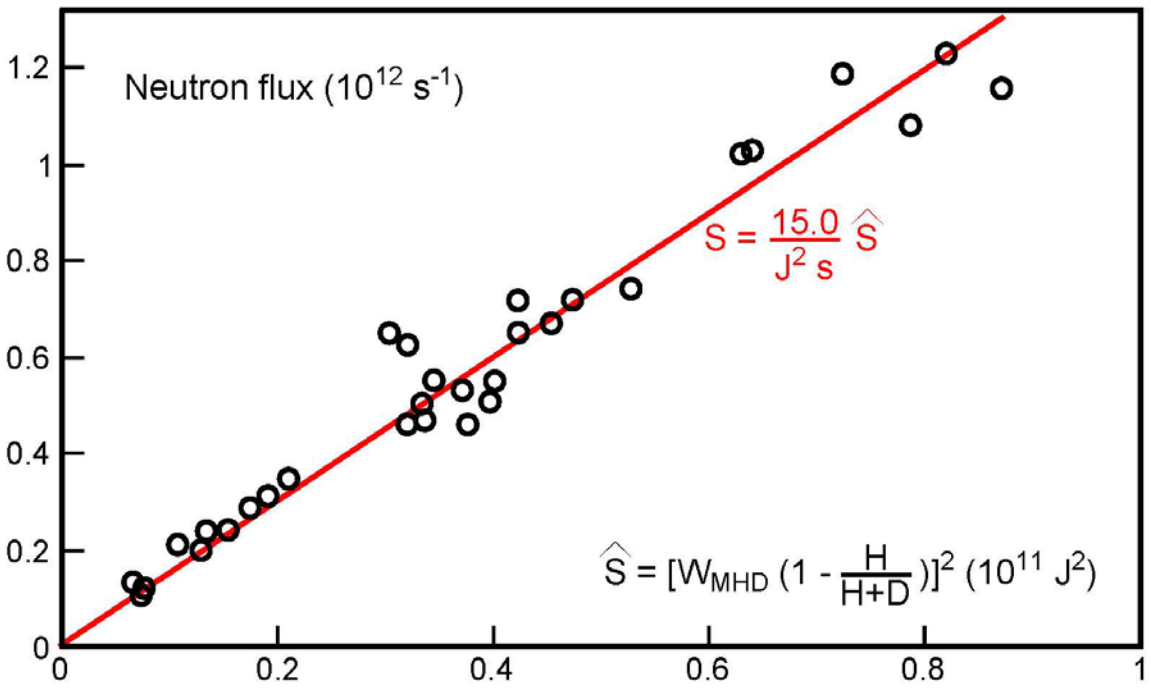

Figure 7: Correlation of the neutron flux with neutron rate as estimated by using the H/(H+D) fraction obtained by divertor spectroscopy measurements. Measured data (black circles) and fit (solid red line).

Apart from the replication data set composed using the total applied particle flux, for any set a strong correlation (between 0.87 and 0.99) is found. For the entire total applied particle flux set, the deviation is caused by the strong wall impact for the low flux and H or D dominated cases as discussed before. Highest correlation has been found for the divertor spectroscopy data set, the corresponding correlation plot is displayed in figure 7. Therefore, the neutron flux (divided by W_{MHD}^2) appears to be good indicator to estimate the H/(H+D) ratio of the plasma for cases with H^0 beams and could be used for feedback control actuation. This can also be seen from the estimated H/(H+D) ratio obtained by reverting the linear regression function, i.e. adopting the measured neutron rate for S as explanatory variable while taking W_{MHD} as a good estimate for the plasma stored energy. Taking $c = 15.0\ \frac{1}{J^2 s}$ for calibration, the data plotted in figure 6 illustrate this procedure in principle.

6. Analysis of the H/(H+D) ratio impact on plasma energy and particle confinement

In order to investigate the impact of the H ratio on the plasma performance, in particular the energy and particle confinement, a dataset was constructed taking advantage of the three HD discharges discussed and three reference shots run entirely with D. While the HD discharges were performed using merely feed-forward pellet and gas flux. Experiments in D employed feed-forward fuelling as well. However, in some phases also density profile control by double feedback on gas and pellets was applied. In all cases, the largest possible pellet size and the same launching speed of 560 m/s was utilised. For the D pellets (with $m_P = 3.7 \times 10^{20}$ D), due to less matter density of H with respect to D the matter flux of HD pellets is about 6% reduced with respect to pure D pellets. Taking into account the fact that transfer losses and delivery efficiency vary, the pellet performance from shot to shot anyway by an at least comparable magnitude, this effect was regarded as marginal. The D reference shots showed outside of the pellet phases a reasonable performance with an energy confinement about 0.95 times the value predicted by the scaling H98(y,2) [W]. There, type-I ELMs with a frequency of typically 50 Hz occurred. With increasing density in the pellet phases, the ELM behaviour changed into a regime with higher frequency and smaller amplitude, while the energy confinement was somewhat reduced. The entire dataset was assembled by recording the values of all characteristic parameters during reasonably steady phases only, i.e. excluding phases with significant transient behaviour. In the HD pellet cases, H/(H+D) values as measured by spectroscopy were adopted, since by this method the best consistency with the neutron rates has been obtained. For the D pellet cases, always H/(H+D) = 0 was set although data showed values up to 0.07.

6.1. Energy confinement

To evaluate the influence of the H ratio on the energy confinement, it turned out to be necessary to take into account the rather strong variation of the plasma energy, estimated here by W_{MHD}, resulting from the differences in total heating power and density. First, the effect of heating power variation was taken into account, as far as possible. For our small dataset, this influence can be seen by plotting W_{MHD} versus the total applied heating power (Ohmic and auxiliary), see figure 8. There, data taken for the HD discharges are represented by the red dots while D reference phases are indicated by the blue dots. Due to the available higher ICRH power, the D reference points cover a much wider range. In order to consider only comparable phases, data with heating power in excess of 9 MW were disregarded for the further analysis in this paper (grey shaded area in figure 8). The remaining D data are fitted (grey solid line) applying a $P^{0.31}$ power dependence, which yields a fair reproduction for the considered power range below 9 MW.

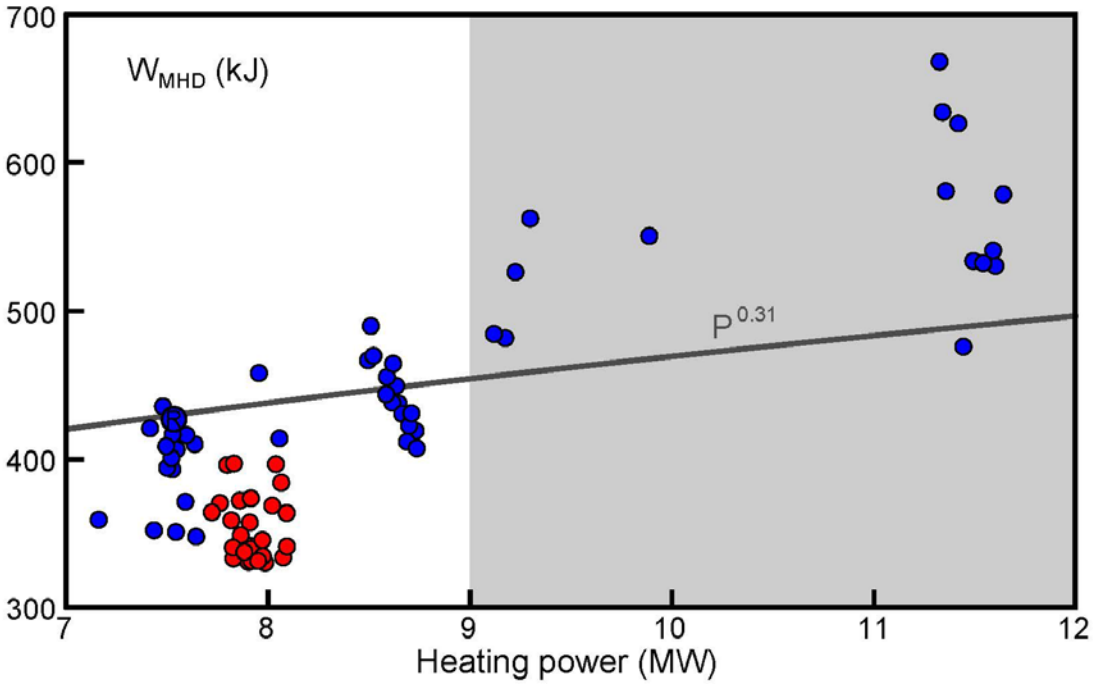

Figure 8: Plasma energy versus applied total heating power for the discharges with HD (red dots) and D (blue dots) pellet injection. Restricting the analysed data set to heating power below 9 MW, the remaining data are normalised by taking the power dependence as predicted by the H98(y,2) scaling. The reference value P_{ref} = 7.528 MW is indicated by "R".

To take into account different P values for the mixed isotope dataset, the W_{MHD} data are normalized with respect to the total applied heating, "ceteris paribus" as,

$$W_{PN} = W\left(\frac{P}{P_{ref.}}\right)^{0.31}$$

An experimental point with P_{ref} = 7.528 MW and W_{MHD} = 417 kJ has been chosen as reference. For this normalization the $P^{-0.69}$ power dependence in the expression for H98(y,2) [W] has been used. (Since we assume a negligible contribution of fast particles in this density regime due to the high collisionality, W_{MHD} is expected to be close to the plasma thermal energy W_{th}.)

Secondly, an attempt was made to eliminate the influence of the density on confinement. The density dependence is visible from figure 9, where W_{PN} is plotted against the obtained central density, as measured by Thomson scattering [X], and normalised to n_{Gw}. It is noted that in these discharges n_{Gw} was very nearly constant; the normalisation with n_{Gw} has been done nevertheless to ease comparison to theory and other experiments. Data from the restricted range in heating power are represented by the same symbols as in figure 8; data as already deselected previously (with heating power above 9 MW) are indicated by black circles. Significantly higher core densities are achieved in the pure D reference discharges, presumably due to a higher particle confinement time as discussed in the following chapter. Again, in order to consider only comparable cases, a further restriction of the dataset was imposed by excluding core densities above $n_{Gw} = \frac{I_P}{\pi a_{min}}$ (indicated by grey shaded area in figure 9). From the figure one can see that in this regime (indicated by the white area) for the D reference discharges W_{PN} decreases with (normalised) central density n_e^0/n_{Gw}. Fitting these data by a simple power law yields W_{PN} proportional either to $n_{e0}^{-0.46}$ or to $(n_e^0/n_{Gw})^{-0.46}$; as indicated by the solid grey line. Above n_{Gw}, W_{PN} remain approximately constant. The dashed

grey line fits the mean value of W_{PN} in the range n_e^0 between 1.0 and 1.82 n_{Gw}. The core density n_e^0 is not a plasma parameter used in the H98(y,2) scaling. In the insert of figure 9 one can see that the peaking factor of $n_e^0/\overline{n_e}$ increase in the region where W_{PN} remains approximately constant. In the region below n_{Gw} it is not clear whether the peaking factor increases but according to the available date it does not seem to decrease. The observed behaviour of W_{PN} with n_e^0 is therefore not expected to be well in agreement with the H98(y,2) scaling, which used $\overline{n_e}$ instead of n_e^0. For the pellet accessed high density regime the scaling is regarded inapplicable anyway since it is well beyond about 0.85 times n_{Gw}, where gas puffing encounters the H-Mode DL [D], pellet fuelling can at best keep the plasma energy constant. The observed declining energy confinement with increasing core density indicates this type of discharge is not optimized for high power density operation.
To take into account the influence of both heating power and density, the normalization (reference point indicated again) finally gets

$$W_{PDN} = W_{ref.} \left(\frac{P}{P_{ref.}}\right)^{0.31} \left(\frac{n_{e0}}{n_{e0\,ref.}}\right)^{-0.46}$$

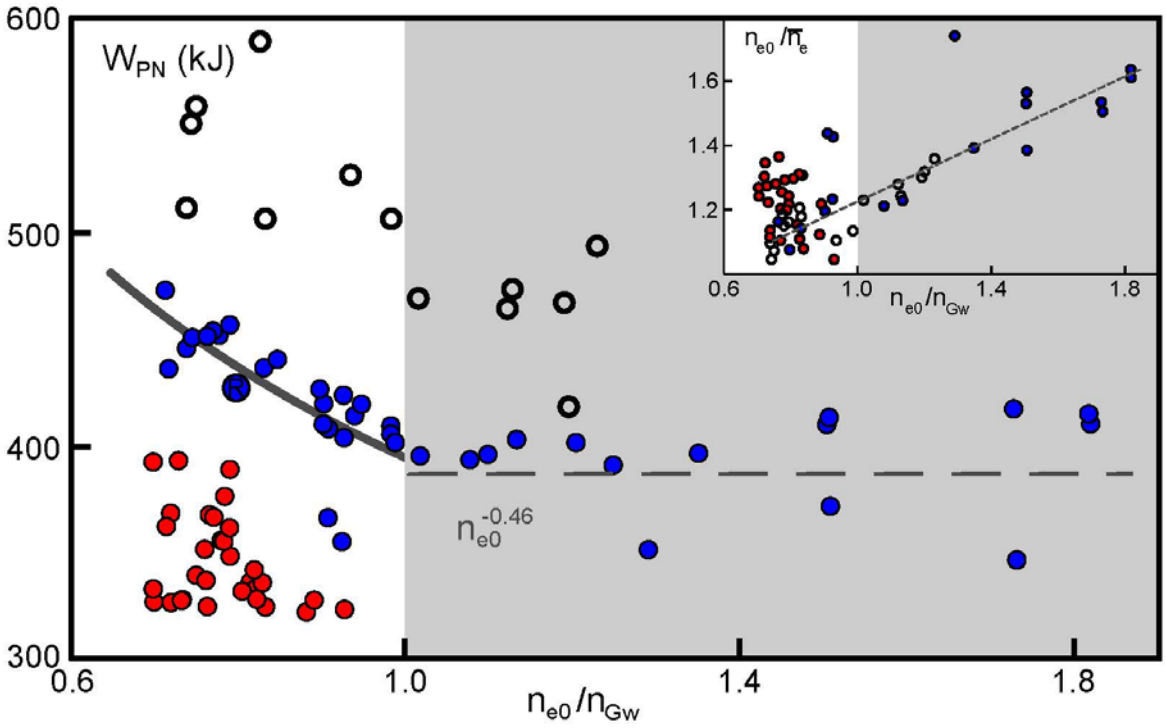

Figure 9: Stored MHD plasma energy normalized with respect to heating power versus core density normalized to the line-averaged Greenwald density formula. The solid line shows a fit to the pure D data from the reference discharges with heating power below 9 MW and core density below n_{Gw}; the dashed line fits the mean value of W_{PN} above n_{Gw}. The inset shows the peaking factor $n_e^0/\overline{n_e}$, the dashed line indicated that the peaking factor increases with the normalised core density for the pure D plasmas.

With this normalisation, the relation between the H ratio on the confinement can be visualised by figure 10, W_{PDN} is plotted versus H/(H+D) for the selected data points. To both the D data (blue dots) and the HD data (red dots) a fit was performed taking, from H98(y,2), the $M^{0.19}$ dependence on the average ion mass M. Clearly, both fits show a significant deviation indicating the absolute influence of H here is approximately M^{a_M} with a point estimate of a_M in the range 0.7 – 0.9. This is considerably more pronounced than predicted by several scaling

expressions such as H93-P, EPS-97 and H98(y,2) as well as than the rather weak isotope dependence observed at JET, see [AG] section 5. Possibly, this can be attributed to the specific scenario. However, in addition it seems there is not a smooth power law-like transition between the half-integer M values. From figure 10 one can see that a significant drop of confinement occurs already when just a small amount of H is added to the initial D plasma. This possibility of one species pulling down energy confinement stronger than anticipated by the scaling needs further investigation, in particular since then the scaling derived for integer M values only no longer holds for intermediate values. As a consequence, for the reactor aiming to operate close to M = 2.5 scaling based reactor modelling could systematically overestimate the expected energy confinement by approximately by some 5% or so.

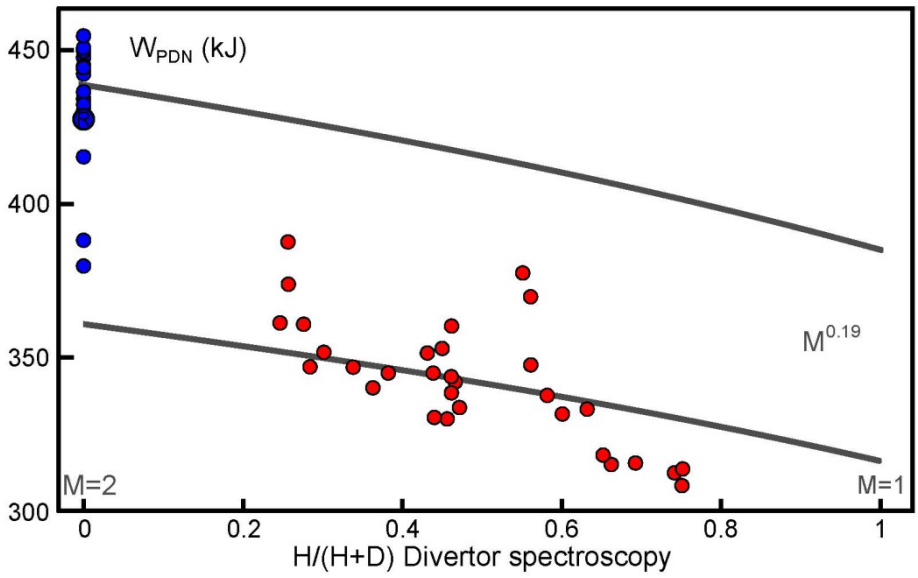

Figure 10: H/(H+D) from divertor spectroscopy versus plasma stored MHD energy normalized with respect to heating power and density dependence. Red dots: H/D pellet fuelled shots. Blue dots: data from reference shot with heating power below 9 MW and core density below n_{Gw}. When attributing D references to M=2 and pure H operation to M=1, it turns out the observed behaviour near H/(H+D) = 0 does not fit well with a simple isotope fraction exponent a_M for some a_M, e.g. $0 < a_M < 1.0$.

6.2. Particle confinement

Already from the D data set extending up to significantly higher densities than the HD data although applied gas and pellet fluxes have been comparable gives an indication of a reduced particle confinement in the presence of H. Hence, a first approach to analyse the particle confinement time τ_P from the fuelling behaviour was performed. This approach takes into account the fuelling efficiency defined as plasma particle inventory N (or central density) enhancement per applied particle flux Γ; hence $\tau_P = \frac{N}{\Gamma}$ respectively $\tau_P = \frac{n_{e0}}{\Gamma}$. However, although the pellet flux into the plasma core is quite precisely known, the influx stemming from gas puffing and wall release is not and hence the precise quantity of Γ. Thus, a precise quantitative result cannot be achieved but a qualitative one from the significant difference observed between D references and HD discharges. This is shown in figure 11, showing a comparison between a pure D plasma (left) and case with H/(H+D) ratio of about 0.6 (right, case with pure H gas puffing). The two cases differ slightly with respect to the applied total heating power (8.6 MW and 8.0 MW), and even stronger with respect to the achieved plasma

energy (boxes b); according energy confinement times estimated to be about 50 ms and 40 ms. Compared to the D reference, more frequent smaller ELMs are observed in the HD case (boxes a). Particle fluxes applied are very similar in both cases (boxes d). Regardless, a striking difference is found for the impact of the fuelling. While a rather strong density build up takes place for the D case only a moderate one is observed in HD discharge (boxes c). Hence, even when taking into account the difference of both discharges, the drastically lower fuelling efficiency strongly indicates for a lower particle confinement in the presence of H with respect to pure D discharges.

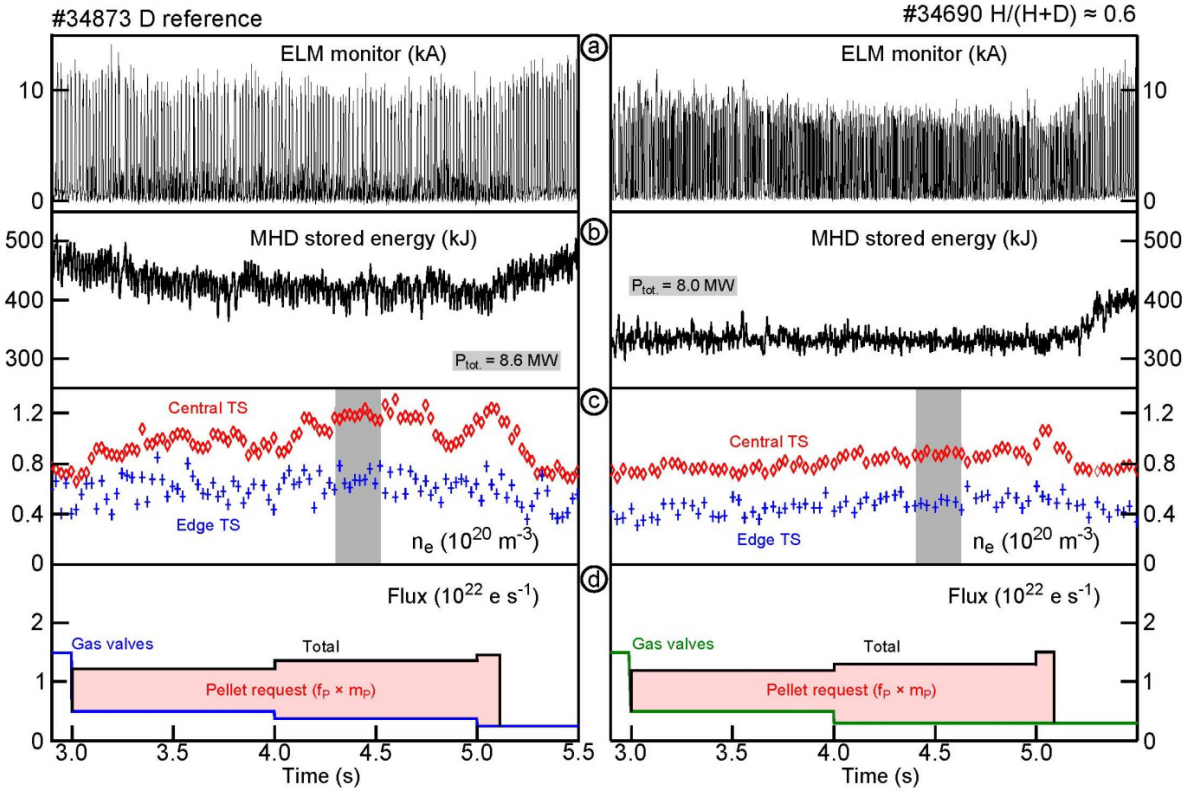

Figure 11: Comparison of the fuelling impact of the pellets in the pure D reference discharge (left) and the discharge with a H/(H+D) fraction of about 0.6 (due to divertor spectroscopy). In both cases, the initiated particle fuelling is almost identical; also the heating power is nearly the same. Obviously, the density increase is much reduced in the presence of H – indicating for a reduction of the particle confinement time. For both cases phases stable with respect to the density evolution are chosen for analysis of the pellet imposed density perturbations (indicated by the grey bars, sequences of pellets with virtually identical size on arrival without lost pellets).

A more quantitative result can be obtained from the temporal evolution of the pellet imposed density perturbation. For this, the pellet particle sustainment time τ_p^* was analysed. This was done for both the D reference and the HD case taking phases without a significant persistent density profile evolution, indicated by the grey shaded areas in the box c of figure 11. In both cases, 11 pellets arriving at 47 Hz result in a similar repetitive temporal perturbation yet keeping a quasi-steady-state situation. Hence, the two pellet ensembles were picked for a statistical analysis comparing the dynamics in particle transport and taking τ_p^* as indicator for τ_p. The result is shown in figure 12. To monitor the evolution of the plasma density, the data from DCN laser interferometer (box a) were taken since only they provide the sufficient temporal resolution. However, since pellet induced fringe jumps falsify the absolute density values, only the relative post pellet density evolution can be taken. Taking the pellet ablation monitor (box b) as synchronization marker, an average over each 11 pellets was performed assume all pellets within one case (but not the two cases) are identical. Fitting an exponential

decay to the resulting averaged post pellet density evolution finally yields the requested pellet particle sustainment time τ_P* for both cases (boxes c). Notably, the confidence range for the fit and hence the uncertainty on τ_P* is largely due to the remaining uncertainty when estimating the unperturbed density base line from Thomson scattering measurements unaffected by the pellet perturbation.
Results show D pellets result in a significantly stronger density increase; this is most likely due to their larger initial particle content but also to much lower transfer losses in the guiding system. Despite the higher plasma energy, D pellets penetrate deeper into the plasma (shown in boxes d are typical ablation radiation measurements for single pellets, the Δt variation refers to the ensembles analyses – assuming pellets move along the designated injection path with constant speed, normalized poloidal positions indicated as well).

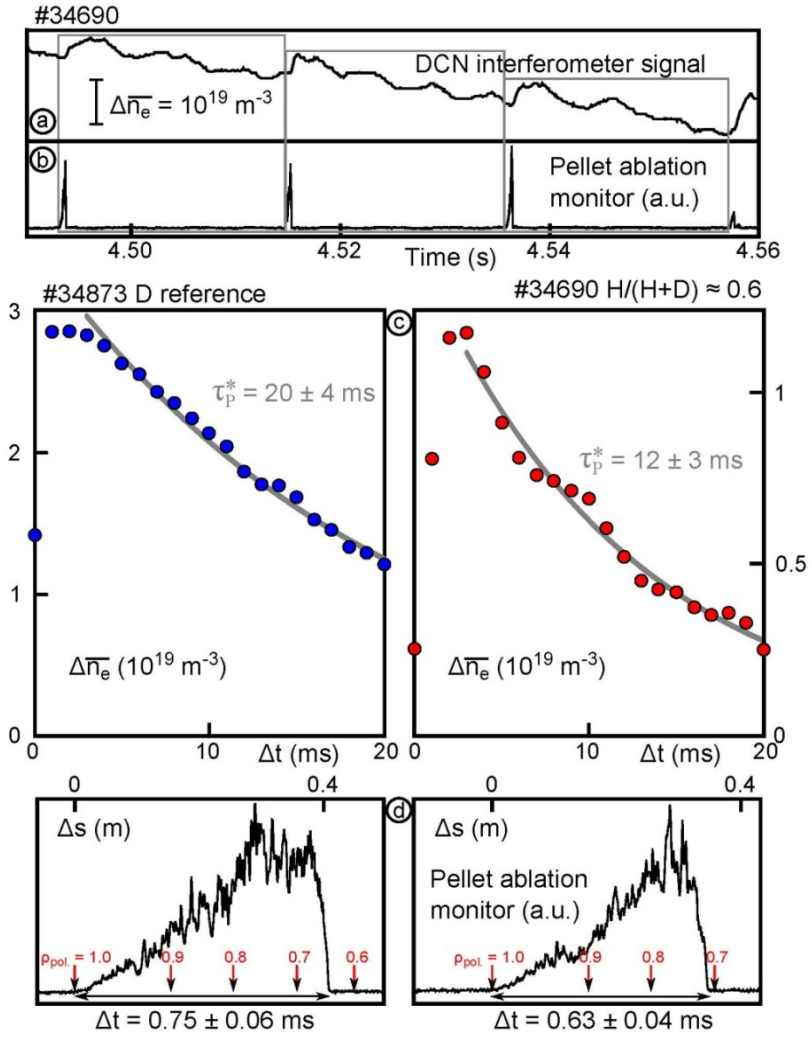

Figure 12: Determination of the pellet particle sustainment time τ_P for a pure D (left) and a HD plasma (right) from the post pellet density decay averaging over 11 virtually identical pellet each (c). Data are taken from the DCN laser interferometer (a) eliminating fringe jump by taking advantage of the pellet ablation monitor as synchronization marker (b) and calibration to Thomson data. D pellets penetrate deeper into the plasma, as shown by typical ablation radiation measurements for single pellets (d).*

The strong reduction of τ_P* provides a clear documentation for the significant reduction of the particle confinement time when D is replaced to a large fraction by H. Taking the relations of

pellet particle sustainment times with respect to the according estimates for the energy confinement times – $\tau_P^* \approx 12$ ms and $\tau_E \approx 40$ ms for H/(H+D) ≈ 0.6, $\tau_P^* \approx 20$ ms and $\tau_E \approx 50$ ms for pure D. The strong variation between the particle replacement time in D and HD and the corresponding - weaker - changes of the energy confinement time suggest turbulence and transport studies which could shed further light on details of the phenomena summarized as isotope effect.

7. Nitrogen doped pellets as subject to test the multi component pellet approach

Beyond its application for high density operation and control of the isotope fraction, an advanced and fully optimized pellet tool can certainly be used for even more applications, for example, the efficient transfer of PEG, gases for radiative power, or of rare and expensive gas species. Efficiency in this context means to achieve the task with a minimum particle flux resulting in a relaxed burden on the exhaust purification system. Moreover, it seems likely that such an approach could also have synergetic effects, fostering the fuelling performance. The admixing of, for example, small amounts of N to the D has been found to harden the ice and consequently the pellet made from this ice. This leads to lower mass losses due to reduced abrasion along the guide pathways in the transfer system [Y]. Doping the fuel can also result in enhanced power dissipation in the ablation cloud surrounding the pellet and by this reduce the power flux to the pellet and hence the ablation rate. Thus, radiative pellet shielding would result in deeper pellet penetration and in turn effectuate a higher fuelling efficiency. Hence, studying pellet actuation with added elements has potential benefits.

In recent experiments the presence of N in the plasma has been found to be advantageous in combination with pellet fuelling to achieve high-density high energy-confinement operation. Furthermore, pellet actuation enhanced the divertor compression of N and thus resulted in better divertor cooling [F]. Hence N was regarded as prime candidate to use as a doping element in pellets. Although there are no known limits to the amount of N that can be added for either the ice formation or pellet handling, for our test technical limitations restricted the N-doping percentage. For the centrifuge acceleration device used, the specific layout of the stop cylinder, which is designed and optimised for pure hydrogen operation, restricts the maximum doping grade to about 1%. Higher amounts increase the ice hardness significantly and were found to cause damage. This restriction would be easy to overcome with an improved set up; however, this was not available at the time of these experiments. Accordingly, the first experiments applying N-doped pellets was performed by producing ice from a gas mixture of D_2 with 1% of added N_2. Again, first the characterisation of the pellet composition was done by injection into the evacuated torus with plasma. The careful comparison of doped and pure D reference pellet injection showed a content of 0.8 % N_2 in the evaporated doped pellet material [Z]. With this basic qualification of the actuator, pellets were injected finally into a suitable available discharge. One should note that this test had to be performed during a set of experiments that introduced N via gas puffing for a different purpose. Since N is sustained in the vessel for several discharges [H] after injection, this caused a significant N background level during these experiments. Nevertheless, the pellet-induced N fuelling could be clearly seen.

An overview of this test discharge is shown in figure 13, which displays from top to bottom: applied auxiliary heating and radiation (a), plasma energy (b), line-averaged and core and edge local densities compared to n_{Gw} (c), the ELMs (d), pellet ablation (e) monitor signals, applied gas and pellet particle fluxes (f), tungsten density (g) and N concentration (h) in the core plasma. Pellet fuelling shows the usual positive impact on the density evolution, namely a high density phase with a central density in the vicinity of $n_{Gw.}$ The enhanced density phase correlates with enhanced ELM activity, slightly higher radiative losses and a mild loss of energy confinement. The enrichment of N by the pellets is also nicely demonstrated concomitant with a drastic reduction of the unwanted tungsten density. Seemingly, the N

content is increased despite an enhanced outward particle flux during the pellet phase due to a higher ELM rate and, possibly, to a reduced particle confinement time.

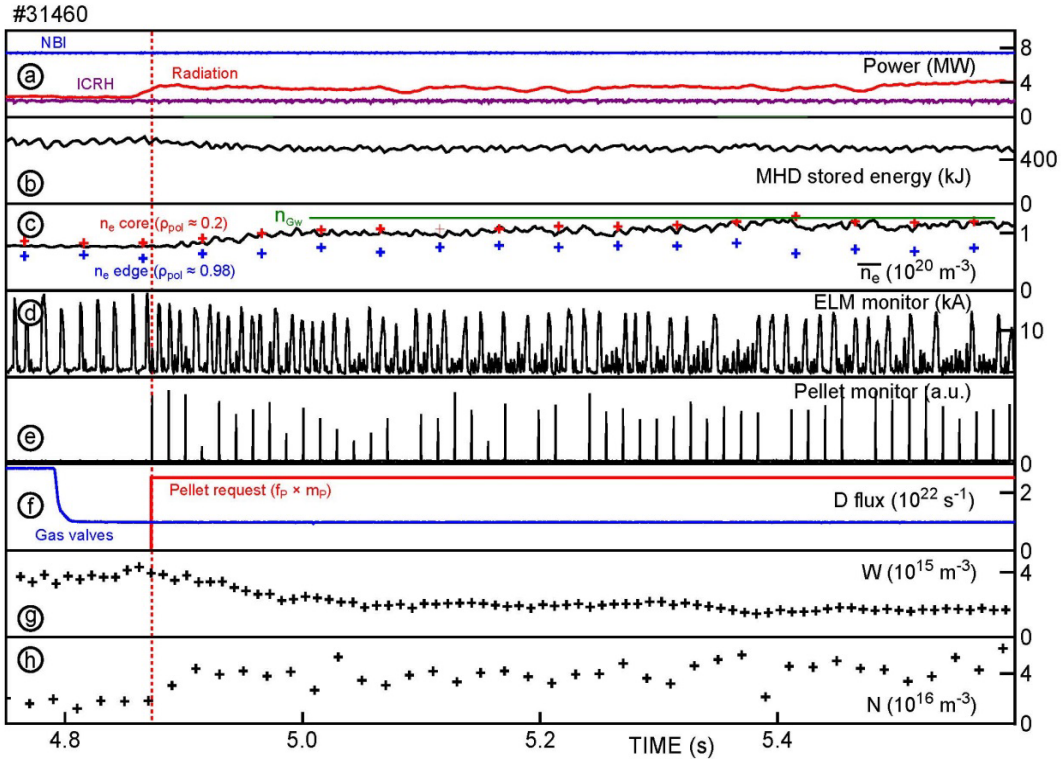

Figure 13: High density operation achieving a core density in the vicinity of n_{Gw} by pellet injection. Doping the D host pellets by N (0.8 % found in the released gas) yields an enhancement of the N concentration in the plasma while the impurity level, here represented by the W concentration, is reduced.

8. Conclusive summary and outlook

The safe and efficient operation of future fusion power plants will require core particle fuelling by pellet injection. In order to fully qualify the pellet tool for the tasks ahead, a couple of technical problems and physics questions still have to be solved. Research and design activities to foster this topic are an essential part of the ASDEX Upgrade research program. In this direction, it has recently been shown [F] that operation at the required high core densities while keeping high confinement can be achieved. To do so, feedback control of the density profile is required. This necessitates the establishment of a set of control parameters that are resilient against the pellet-imposed perturbations. As a next continuative step, experiments aimed at incorporating the plasma isotope mixture into this control scheme were performed, and presented in this work. For this purpose, it is evidentially necessary to further investigate e.g. observed discrepancies between the NPA measurements and the simple neutron model used by more sophisticated modelling of the neutron fluxes.

Our proposed scheme to control the plasma isotope mixture in a future fusion reactor suggests a direct control via adjustment of the pellet isotopic mixture. Since for this scheme, a single pellet train is already sufficient; the necessary technological effort can be kept rather low. Following this approach, in a reactor both density and isotopic mixture in the core would be controlled by this single pellet train. While the density would be adapted on a shorter time scale by controlling the pellet rate and hence the flux, the DT mix in the core, possibly monitored by the fusion output power, would be matched by the DT mix of the pellets on a longer time scale. This is quite different with respect to the original plans of ITER, which aimed at controlling both quantities by combining two pellet trains, one formed from D or D

enriched pellets and the other of T or T enriched pellets. Recently, modelling investigations [AB] showed difficulties for achieving a stable isotope core mix by employing such a combination of two pellet trains.
In our experiments, the reactor-relevant mix of DT was mimicked by the use of HD. Successful reliable and reproducible formation of HD pellets with the desired isotope mixture was achieved; these pellets were applied for a demonstration of the envisaged plasma isotopic mixture control. However, it turned out that additional efforts are still needed in order to allow for a reliable real-time diagnosis of the core isotope mixture. Valuable data were derived as a spin-off of the control experiments, indicating that H in D reduces the energy confinement, potentially already significantly when yet present at a small ratio. The latter might emerge a potential deficiency when using a simple factor M^{a_M} for the isotope effect, which was done with $a_M = 0.19$ in H98(y,2).
Also, H in D reduces the particle confinement; this effect presumably is even stronger than the impact on the energy confinement. As a result of the particle confinement lowered in comparison to pure D reference plasmas, HD pellet actuation thus results in less density build up and a significantly faster decay of pellet imposed density surplus. Due to the technology optimised approach, results are providing a rather qualitative indication yet. However, the experiments also demonstrate the potential use of the pellets in experiments planned aiming on dedicated physics, e.g. by allowing for a detailed insight into the particle dynamics by analysing of the pellet particle sustainment time or by introducing precisely dosed amounts of H to investigate the confinement evolution with increasing small amounts of H. Continuation of the presented investigation by such experiments have been indeed already in preparation when the AUG campaign 2017 was forced stopped by a major technical problem and this program become subject to a major postponement. Once HD pellet experiments can be resumed, it is also planned to combine isotope mixture control with feedback controlled operation aiming to achieve simultaneously high density and high confinement, sounding out the capabilities of different plasma scenarios and regimes for this goal. Hence, the pellet tool can become quite serviceable for the investigation of the isotope effect. In agreement with our findings, the isotope effect on confinement has been found favourable with respect to increasing M. According findings are reported from many devices and are attributed to multifaceted physics effects [AC, AD, AE].
Beyond their fitness to serve standard fuelling tasks, pellets have been also tested to act as host for other gases employed for different accessory tasks as e.g. plasma performance enhancement, radiative cooling, divertor buffering or enhancement of plasma heating schemes. By doing so, it became conceivable possibly synergetic effects can boost both the efficiency for supplying the added material and the fuel, the latter potentially also benefitting from pellet hardens and penetration enhancement due to radiative pellet shielding. Despite the technical limitation of our system layout not foreseeing this kind of operation restricting the amount of added material, first tests with N have shown already very encouraging results. Further investigations are considered respectively already in preparation as e.g. solving small amounts of the prized ^{3}He reported feasible [S] in order to assist for the ‘three-ion’ heating scenario [AF].

Acknowledgment
This work has been carried out within the framework of the EUROfusion Consortium and has received funding from the Euratom research and training programme 2014–2018 under grant agreement No 633053. The views and opinions expressed herein do not necessarily reflect those of the European Commission.

References

[A] R. Wenninger et al., Nucl. Fusion 57 (2017) 016011
[B] P.T. Lang et al., Fusion Eng. Design 96-97 (2015) 123
[C] M. Greenwald et al., Nucl. Fusion 28, 2199 (1988)
[D] M. Bernert et al., Plasma Phys. Control. Fusion 57 (2015) 014038
[E]T.H. Osborne et al., Phys. Plasmas 8 (2001) 2017
[F] P.T. Lang et al., Nucl. Fusion 58 (2018), 036001
[G] Y. N. Hörstensmeyer, B. Butler, Ch. Day, F. Franza, Fusion Eng. Design (2018), https://doi.org/10.1016/j.fusengdes.2018.02.015
[H] M.G. Dunne et. al, Plasma Phys. Control. Fusion 59 (2017) 014017
[I] C. Andelfinger et al., Rev. Sci. Instrum. 63 (1993) 983
[J] B. Ploeckl et al., Fusion Eng. Design 88 (2013) 1059
[K] D. Neuwirth, V. Rohde, T. Schwarz-Selinger and ASDEX Upgrade Team, Plasma Phys. Control. Fusion 54 (2012) 085008
[L] A. Drenik, Fusion Eng Des. 124 (2017) 239
[M] G.L Price and E. Iglesia, Ind. Eng. Chem. Res. 28 (1989) 839
[N] S. Potzel et. al, Nuclear Fusion 54 (2014) 013001
[O] Bartiromo et al., Rev. Sci. Instrum. 58, 788 (1987)
[P] P.A. Schneider et al., Rev. Sci. Instr. 86 (2015) 073508
[Q] Geiger et al., Plasma Phys. Controlled Fusion 53 (2011) 65010
[R] G. Tardini et al., Nucl. Fusion 53 (2013) 063027
[S] P.C. Sours, “Hydrogen properties for fusion energy”, University of California press (1986)
[T] C.J. Rapson et al., Fusion Eng. Des. 123 (2017) 603
[U] D. Strachan et al., Nucl. Fusion 33 (1993) 991
[V] O.J.W.F. Kardaun, “Classical Methods of Statistics”, Springer-Verlag Berlin Heidelberg 2005, page 102
[W] ITER EXPERT GROUPS, et al, Nucl. Fusion 39 (1999), 2175
[X] B. Kurzan and H.D. Murmann, Rev. Sci. Instr. 82 (2011) 103501
[Y] P.T. Lang et al., Nucl. Fusion 42 (2002), 388
[Z] B. Ploeckl et al., Fusion Engineering and Design 96–97 (2015) 155
[AB] A. Polevoi et al., „Integrated modelling of ITER scenarios with D-T Mix control“, EPS 2018 Prague
[AC] C.F. Maggi et al., Plasma Phys. Control. Fusion 60 (2018) 014045
[AD] F. Laggner et al., Phys. Plasmas 24 (2017) 56105
[AE] P.A. Schneider et al., Nucl. Fusion 57 (2017), 066003
[AF] Ye. O. Kazakov et al., Nat. Phys. 13 (2017) 973
[AG] The JET Team (presented by K. Thomsen), Plasma Phys. Control. Fusion 41 (1999) A617